Some theoretical comments regarding the run-length properties of the synthetic and runs-rules $\bar{X}$ monitoring schemes – Part 1: Zero-state

Sandile C. Shongwe*
Department of Statistics
Faculty of Natural and Agricultural Sciences
University of Pretoria
Pretoria
South Africa

Marien A. Graham
Department of Science, Mathematics & Technology Education
Faculty of Education
University of Pretoria
Pretoria
South Africa

Abstract

In this paper, we discuss the short-term (also known as zero-state mode) run-length theoretical properties of the four different types of synthetic and runs-rules $\bar{X}$ monitoring schemes that were empirically analyzed in another paper. That is, we provide and point out how each corresponding type of the *2-of-(H+1)* runs-rules and synthetic charts' transition probabilities matrices (TPMs) differ from each other in zero-state, for any positive integer *H*. Next, using these general TPMs and the standard Markov chain formulae, we derive the general form of the average run-length (*ARL*) vectors and the corresponding zero-state *ARL* expressions for any shift value for each of the four different types of the synthetic and runs-rules $\bar{X}$ monitoring schemes. Finally, we provide expressions to calculate the overall run-length performance for each of the schemes. While there is lots of literature available on empirical analysis of zero-state synthetic and runs-rules charts, there is very little on the corresponding theoretical analysis. We believe this paper will, in some part, fill this gap and encourage more research in this area.
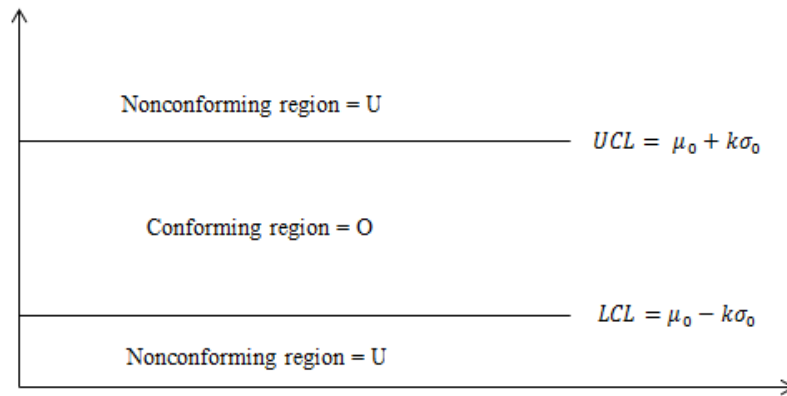
1. Introduction

The basic theory of statistical process control and monitoring (SPCM) was developed in the late 1920's by Dr. W. Shewhart, and was popularized worldwide by Dr. W.E. Deming – see for instance, Montgomery (2013) and Qiu (2014) for more details on the early development in the area of SPCM. According to Benneyan et al. (2003), Dr. Shewhart originally worked with manufacturing processes; however, he and Dr. Deming quickly realized that SPCM could be applied to a number of other processes. Wisner (2009) stated that SPCM is not merely a set of statistical tools but a management philosophy that helps organizations to improve performance and sustain high productivity. In an effort to improve productivity and reduce waste, supplementary runs-rules and synthetic $\bar{X}$ monitoring schemes have been proposed in the literature to improve the performance of the basic Shewhart $\bar{X}$ chart in detecting small and moderate shifts in a process for normally distributed observations. A *w-of-(w+v)* runs-rules chart is a monitoring scheme that requires at least *w* out of the last *w+v* consecutive plotting statistics to fall beyond the control limits before issuing an out-of-control (OOC) signal, where *w* and *v*
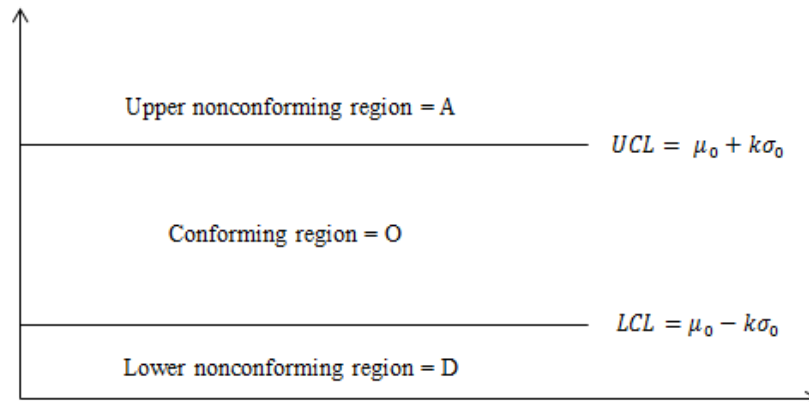
---

* Corresponding author: S.C. Shongwe (sandile@tuks.co.za)

are integers, with $w \geq 2$ and $v \geq 0$, see the review by Koutras et al. (2007). A synthetic chart is a monitoring scheme that combines the operation of the basic $\bar{X}$ chart and the conforming run-length (*CRL*) chart; see Wu and Spedding (2000), the review by Khoo (2013) and some more recent publications, for example, Haq and Khoo (2016) and Shongwe and Graham (2018). Bourke (1991) defined a *CRL* chart as a monitoring scheme that plots the number of conforming samples between two nonconforming samples, inclusive of the nonconforming sample at the end. A *CRL* chart signals when a plotting statistic is greater or equal to the control limit, denoted by *H*, i.e. an integer greater or equal to 1. The connection between the runs-rules and synthetic charts was first pointed out by Davis and Woodall (2002), where the authors noticed that a synthetic chart is actually a *2-of-(H+1)* runs-rules chart with a head-start feature. A head-start feature implies that we assume that the first sample is nonconforming; consequently, we need at least one other nonconforming sample within the next *H* plotting statistics for a *2-of-(H+1)* runs-rules scheme to issue a signal. The Shewhart-type synthetic and runs-rules charts can be classified into four different types i.e. non-side-sensitive (NSS), standard side-sensitive (SSS), revised side-sensitive (RSS) and modified side-sensitive (MSS). These four charting regions are as shown in Figure 1 (where *UCL*, *LCL* and *CL* denote the upper control limit, lower control limit and center line, respectively).

The NSS, SSS, RSS and MSS synthetic charts were proposed by Wu and Spedding (2000), Davis and Woodall (2002), Machado and Costa (2014) and Shongwe and Graham (2018) – we denote these by S1, S2, S3 and S4, respectively. The NSS, SSS, RSS and MSS runs-rules charts were proposed by Derman and Ross (1997), Klein (2000), (discussed in) Shongwe and Graham (2018) and Antzoulakos and Rakitzis (2008) – we denote these by RR1, RR2, RR3 and RR4, respectively. The operations of the different synthetic and runs-rules $\bar{X}$ schemes are outlined in Tables 1 and 2, respectively. Since some of the operational elements of the synthetic and runs-rules charts are similar, in Table 2, we only listed those steps with operational elements that are different and the rest are the same as those given in Table 1. For a fair comparison with synthetic charts, moving forth, we only consider runs-rules with $w = 2$, so that $v = H\text{-}1$.

(a) Non-side-sensitive (NSS) regions

Nonconforming region = U

$UCL = \mu_0 + k\sigma_0$

Conforming region = O

$LCL = \mu_0 - k\sigma_0$

Nonconforming region = U

(b) Standard / Revised side-sensitive (SSS / RSS) regions

Upper nonconforming region = A

$UCL = \mu_0 + k\sigma_0$

Conforming region = O

$LCL = \mu_0 - k\sigma_0$

Lower nonconforming region = D
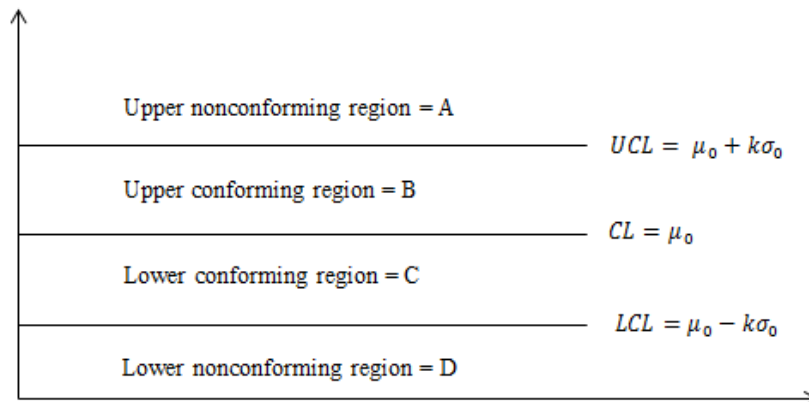
(c) Modified side-sensitive (MSS) regions

Upper nonconforming region = A

$UCL = \mu_0 + k\sigma_0$

Upper conforming region = B

$CL = \mu_0$

Lower conforming region = C

$LCL = \mu_0 - k\sigma_0$

Lower nonconforming region = D

Figure 1: Charting regions of the different types of synthetic and runs-rules schemes

Table 1: Operation of the four different synthetic $\bar{X}$ charts

Step	S1 scheme	S2 scheme	S3 scheme	S4 scheme
(1)	Set the control limit of the *CRL* sub-chart (i.e. *H*).			
(2)	Compute the corresponding k so that the target ARL_0 is attained. Hence the control limits of the $\bar{X}$ sub-chart are $UCL/LCL = \mu_0 \pm k\sigma_0$.			
(3)	Wait until the next inspection time, take a random sample of size n and calculate the sample mean $\bar{X}_i$.			
(4)	If $LCL < \bar{X}_i < UCL$, the ith sample is conforming, hence return to Step (3); otherwise go to Step (5).			
(5)	If $\bar{X}_i \leq LCL$ or $\bar{X}_i \geq UCL$ go to Step (6).	If $\bar{X}_i \leq LCL$ go to Step (6a), or if $\bar{X}_i \geq UCL$ go to Step (6b).	If $\bar{X}_i \leq LCL$ go to Step (6a), or if $\bar{X}_i \geq UCL$ go to Step (6b).	If $\bar{X}_i \leq LCL$ go to Step (6a), or if $\bar{X}_i \geq UCL$ go to Step (6b).
(6)	Calculate CRL^{S1} and if $CRL^{S1} \leq H$ go to Step (7); otherwise return to Step (3).	(6a) Calculate CRL_L^{S2} and if $CRL_L^{S2} \leq H$ go to Step (7); otherwise return to Step (3). (6b) Calculate CRL_U^{S2} and if $CRL_U^{S2} \leq H$ go to Step (7); otherwise return to Step (3).	(6a) Calculate CRL_L^{S3} and if $CRL_L^{S3} \leq H$ go to Step (7); otherwise return to Step (3). (6b) Calculate CRL_U^{S3} and if $CRL_U^{S3} \leq H$ go to Step (7); otherwise return to Step (3).	(6a) Calculate CRL_L^{S4} and if $CRL_L^{S4} \leq H$ go to Step (7); otherwise return to Step (3). (6b) Compute CRL_U^{S4} and if $CRL_U^{S4} \leq H$ go to Step (7); otherwise return to Step (3).
(7)	Issue an OOC signal and then take necessary corrective action to find and remove the assignable causes. Then return to Step (3).			

CRL^{S1}: Number of *conforming* samples that fall in region 'O'; which are in between any two consecutive nonconforming samples that fall on region 'U', see Figure 1(a).

CRL_L^{S2}: Number of (either *conforming* or *nonconforming*) samples that fall in regions 'O' and 'A'; which are in between the two consecutive nonconforming samples that fall on region 'D', see Figure 1(b).

CRL_U^{S2}: Number of (either *conforming* or *nonconforming*) samples that fall in regions 'O' and 'D'; which are in between the two consecutive nonconforming samples that fall on region 'A', see Figure 1(b).

CRL_L^{S3}: Number of *conforming* samples that fall in region 'O'; which are in between the two consecutive nonconforming samples that fall on region 'D', see Figure 1(b).

CRL_U^{S3}: Number of *conforming* samples that fall in region 'O'; which are in between the two consecutive nonconforming samples that fall on region 'A', see Figure 1(b).

CRL_L^{S4}: Number of *conforming* samples that fall in region 'C'; which are in between the two consecutive nonconforming samples that fall on region 'D', see Figure 1(c).

CRL_U^{S4}: Number of *conforming* samples that fall in region 'B'; which are in between the two consecutive nonconforming samples that fall on region 'A', see Figure 1(c).

Note that each computation of the *CRL* value above, includes the nonconforming sample at the end, so that the absence of any nonconforming sample means $CRL = 1$.

Table 2: Operation of the four different *w-of-*($w+v$) runs-rules $\bar{X}$ charts

Step	RR1 scheme	RR2 scheme	RR3 scheme	RR4 scheme
(1)	Specify the desired values of *w* and *v*.			
(6)	*Out of the next* ($w+v-1$) *consecutive samples* – consider Figures 1(a), (b), (c): If ($w-1$) nonconforming samples fall in region U which are separated by *v* conforming samples in region O, go to Step (7); otherwise return to Step (3).	(6a) If ($w-1$) nonconforming samples fall in region D and are separated by at most *v* samples (conforming or nonconforming) that fall in regions O and A, go to Step (7); otherwise return to Step (3). (6b) If ($w-1$) nonconforming samples fall in region A and are separated by at most *v* samples (conforming or nonconforming) that fall in regions O and D, go to Step (7); otherwise return to Step (3).	(6a) If ($w-1$) nonconforming samples fall in region D and are separated by at most *v* conforming samples that fall in region O, then go to Step (7); otherwise return to Step (3). (6b) If ($w-1$) nonconforming samples fall in region A and are separated by at most *v* conforming samples that fall in region O, then go to Step (7); otherwise return to Step (3).	(6a) If ($w-1$) nonconforming samples fall in region D and are separated by at most *v* conforming samples that fall in region C, then go to Step (7); otherwise return to Step (3). (6b) If ($w-1$) nonconforming samples fall in region A and are separated by at most *v* conforming samples that fall in region B, then go to Step (7); otherwise return to Step (3).
	- See Figure 1(a)	- See Figure 1(b)	- See Figure 1(b)	- See Figure 1(c)

A control chart is usually evaluated using either a zero-state or the steady-state run-length properties. In this paper (i.e. Part I), we focus on the zero-state mode and the steady-state mode has been investigated and reported in Part II of this work. A zero-state mode is used to characterize short term run-length properties of a monitoring scheme. Hence, the zero-state run-length is the number of sampling points at which the chart first signals given it begins in some specific initial state and it is assumed that the mean shift always takes place at the beginning of the process, see Zhang and Wu (2005). So, under this assumption, and also assuming that the mean is a fixed and known quantity, the most used quantity in SPCM, to measure the performance of a specific size of a shift (δ), is the zero-state average run-length (*ZSARL*), which is given by

$$ZSARL(\delta) = \mathbf{q}_{(1 \times M)} \cdot \boldsymbol{ARL}_{(M \times 1)}(\delta) = \mathbf{q}_{(1 \times M)} \cdot (\mathbf{I}_{(M \times M)} - \mathbf{Q}(\delta)_{(M \times M)})^{-1} \cdot \mathbf{1}_{(M \times 1)} \tag{1}$$

where $\mathbf{q}_{(1 \times M)}$ and $\boldsymbol{ARL}_{(M \times 1)}$ are the zero-state initial probabilities and *ARL* vectors, respectively, with $\mathbf{I}_{(M \times M)}$, an identity matrix, $\mathbf{1}_{(M \times 1)}$ a vector of ones and $\mathbf{Q}(\delta)_{(M \times M)}$, an essential transition probability matrix (TPM) at some specific size of δ and M is the dimension of the essential TPM discussed in Section 2.

More recently, a number of researchers (see Reynolds and Lou (2010), Ryu et al. (2010), Machado and Costa (2014), Huh (2014, Chapter 4) and some of the references therein) have argued that, if a control chart is designed based on one specific size of a shift, say by means of Equation (1), it would perform poorly when the actual size of a mean shift is significantly different from the assumed size. Thus, they instead recommended that monitoring schemes should be designed in terms of the overall performance run-length metric. Such overall performance run-length functions are called quality loss functions. A quality loss function depicts a relationship between the shift size and the quality loss. That is, the lower the quality loss function value, the better is that particular monitoring scheme. Ryu et al. (2010) observed the uncertainty in δ, and hence, they designed their monitoring scheme to rather minimize quality loss, which is measured by a quantity called the expected weighted run-length (*EWRL*) which is given by

$$EWRL = E[w(\delta) \times ARL(\delta)] = \int_{\delta_{min}}^{\delta_{max}} \left(w(\delta) \times ARL(\delta) \right) \times f(\delta) d\delta \tag{2}$$

where δ follows some probability distribution function with a density function $f(\delta)$ and a range [δ_{min}, δ_{max}], where δ_{min} and δ_{max} are the lower and upper bound of the range of δ, and $w(\delta)$ is a weight function associated with δ.

Note that the *EWRL* in Equation (2) is a generalized quality loss function and when we assign different weight functions, it yields the following different common quality loss function names: (i) extra

quadratic loss (*EQL*) if $w(\delta) = \delta^2$, (ii) expected *ARL* if $w(\delta) = 1$, (iii) expected / average relative *ARL* (*ERARL* / *ARARL*) if $w(\delta) = \frac{1}{ARL_{\text{opt}}(\delta)}$, where $ARL_{\text{opt}}(\delta)$ is the *ARL* at a given δ for some other specified benchmark monitoring scheme; etc. While Ryu et al. (2010) had used the *EWRL* function as a design function, Shongwe and Graham (2018) had used it to compute the *EQL*, *ARARL* and the performance comparison index (*PCI*, which is the ratio of the *EQL* of some competing scheme and the *EQL* of the specified benchmark scheme) and implemented these as an additional evaluation tool. Although it is not the scope of this paper, it is worth mentioning that the effectiveness of traditional performance measures should be revisited. Even as far back as 1986, Woodall (1986) had started to highlight weaknesses in the designs of control charts and there is still room for improvement. We do not wish to degrade the significance of traditional control charting performance measuring techniques, however, the key common characteristic of these previous methods is to keep the control charting design parameters (including δ) fixed and recent literature is now advocating the use of newer, more flexible, performance measures. The exploration into the fact that making use of traditional measures can be misleading is currently under investigation and will be reported on in a separate paper.

In this paper, we make a further contribution to the theory of zero-state synthetic and runs-rules $\bar{X}$ monitoring schemes by:

i.   Giving the general form of each of the scheme's TPM for any $H > 0$;

ii.   We derive the zero-state closed-form expressions of $\mathbf{q}_{(1 \times M)}$ and $\boldsymbol{ARL}_{(M \times 1)}$, so that we formulate the zero-state *ARL* and *EWRL* expressions.

The rest of the paper is organized as follows: In Section 2, we describe the Markov chain imbedding technique and give the general form of the TPMs for each of the schemes. In Section 3, we provide the general form of the *ARL* vectors for each scheme. In Sections 4 and 5, we derive the zero-state run-length characteristics pertaining to synthetic and runs-rules charts, respectively. Overall performance measures pertaining to Eq. (2) are discussed in Section 6. For a build-up to Part II of this work, in Section 7, we give discuss the importance of understand both the zero-state and the steady-state modes. Finally, in Sections 8 and 9, we give some concluding remarks and future recommendations, respectively.

2. General transition probability matrices (TPMs)

To construct the TPMs using a Markov chain imbedding technique, we need to first define the absorbing simple patterns that result in an OOC event as this denotes the waiting time (denoted by *W*) until the first occurrence of an OOC signal, see Fu and Lou (2003). Then from the distinct absorbing simple patterns, we need to extract the corresponding distinct non-absorbing sub-patterns as well as

clearly define the initial state. Therefore, the state space (denoted by Ω) of the Markov chain imbedding technique is made up of three components:

(i) *absorbing state* (i.e. the union of all possible absorbing simple patterns) - in order to reduce the dimension of the TPM for the components corresponding to the states which signal the entrance of the Markov chain to each of the distinct simple absorbing patterns may be substituted by 'OOC';

(ii) *sub-patterns* of the absorbing states;

(iii) *IC conforming region state* i.e. the sub-patterns that denotes the IC conforming region in Figure 1.

Once the three components of the state space have been clearly defined, then for any positive integer M, the TPM is given by

$$P_{(M+1)\times(M+1)} = \begin{pmatrix} Q_{(M\times M)} & | & r_{(M\times 1)} \\ - & - & - \\ 0'_{(1\times M)} & | & 1_{(1\times 1)} \end{pmatrix} \tag{3}$$

where the vector $r_{(M\times 1)}$ satisfies $r = 1 - Q1$ with $1_{(M\times 1)} = (1\ 1\ ...\ 1)'$, $0_{(M\times 1)} = (0\ 0\ ...\ 0)'$. The elements of the TPM in Equation (3) are computed using the probabilities of the plotting statistics falling in each of the regions given in Figure 1. That is, let $\{\bar{X}_i; i = 1, 2,...\}$ be a sequence of i.i.d. trials taking values in the set $\zeta_1 = \{O, U\}$, $\zeta_2 = \{A, O, D\}$ and $\zeta_3 = \{A, B, C, D\}$ for the (RR1, S1), (RR2, S2, RR3, S3) and (RR4, S4) schemes, respectively. Suppose that the values of μ_0 and σ_0^2 are known, then the probabilities of a plotting statistic falling in a specific region are given by

$$p_A(\delta) = Pr(\bar{X}_i \in A) = Pr(\bar{X} \geq UCL) = 1 - \Phi(k - \delta\sqrt{n}),$$

$$p_B(\delta) = Pr(\bar{X}_i \in B) = Pr(CL \leq \bar{X} < UCL) = \Phi(k - \delta\sqrt{n}) - \Phi(-\delta\sqrt{n}),$$

$$p_C(\delta) = Pr(\bar{X}_i \in C) = Pr(LCL < \bar{X} \leq CL) = \Phi(-\delta\sqrt{n}) - \Phi(-k - \delta\sqrt{n}),$$

$$p_D(\delta) = Pr(\bar{X}_i \in D) = Pr(\bar{X} \leq LCL) = \Phi(-k - \delta\sqrt{n}), \tag{4}$$

$$p_O(\delta) = Pr(\bar{X}_i \in O) = Pr(LCL < \bar{X} < UCL) = p_B(\delta) + p_C(\delta), \text{ i.e. 'O'} \equiv \text{'B} \cup \text{C'},$$

$$p_U(\delta) = Pr(\bar{X}_i \in U) = Pr(\bar{X} \geq UCL) + Pr(\bar{X} \leq LCL) = \theta_A(\delta) + \theta_D(\delta), \text{ i.e. 'U'} \equiv \text{'A} \cup \text{D'},$$

respectively; where $\Phi(\cdot)$ denotes the cumulative distribution function (cdf) of the standard normal distribution, δ is the shift parameter expressed in terms of the standard deviation units, n is the sample size. To preserve writing space, we denote '$p_A(\delta)$' by 'p_A' without writing the 'δ' – this is done throughout the whole paper.

Suppose that the sequences of conforming and nonconforming samples, say Λ_t = ABBA, to be the tth simple pattern denoting a sequence of states shown in Figure 1. Then, we define Λ as a compound

pattern if it is the union of ω distinct simple patterns i.e. $\Lambda = \Lambda_1 \cup \Lambda_2 \cup \ldots \cup \Lambda_\omega$. Next, given that an absorbing simple pattern is given by $\Lambda_1=\{ABBA\}$ then the corresponding non-absorbing sub-pattern is given by $\eta_1=\{ABB\}$. Let W denote the waiting time for the first occurrence of Λ, i.e. the waiting time until the first occurrence of one of the patterns, $\Lambda_1,\ldots, \Lambda_\omega$. Hence, $\eta_1,\ldots, \eta_\tau$ are the distinct sub-patterns of the simple absorbing patterns $\Lambda_1,\ldots, \Lambda_\omega$, without the last element, where $\tau \leq \omega$. Note that one of these η_i is equal to the transient state, denoted by ϕ, corresponding to the IC conforming region in Figure 1 for each respective chart. Thus, for the runs-rules charts, the Ω is made up of: (i) 'OOC' $\equiv$ $\Lambda_1,\ldots, \Lambda_\omega$; (ii) the sub-patterns i.e. $\eta_1,\ldots, \eta_\tau$; (iii) the IC conforming region state, ϕ.

Table 3: Components of the state space of the *2-of-(H+1)* runs-rules and synthetic $\bar{X}$ charts when $H =$ 1 and 2

H	Type	Λ	Ψ	ϕ	η	ψ	Ω
1	RR1 S1	$\Lambda_1=\{UU\}$	None	$\eta_1=\{O\}$	$\eta_2=\{U\}$	None	$\{\phi,\eta_2;OOC\}$
	RR2 RR3 RR4	$\Lambda_1=\{AA\}, \Lambda_2=\{DD\}$	None	$\eta_2=\{O\}$ / $\eta_2=\{B,C\}$	$\eta_1=\{A\}, \eta_3=\{D\}$	None	$\{\eta_1,\phi,\eta_3;OOC\}$
	S2 S3 S4	$\Lambda_1=\{AA\}, \Lambda_2=\{DD\}$	$\Psi_1=\{\pm A\},$ $\Psi_2=\{\pm D\}$	$\eta_2=\{O\}$ / $\eta_2=\{B,C\}$	$\eta_1=\{A\}, \eta_3=\{D\}$	$\psi_1=\{\pm\}$	$\{\eta_1,\phi,\eta_3;\psi_1;OOC\}$
2	RR1 S1	$\Lambda_1=\{UU\}, \Lambda_2=\{UOU\}$	None	$\eta_1=\{O\}$	$\eta_2=\{U\}, \eta_3=\{UO\}$	None	$\{\phi,\eta_2,\eta_3;OOC\}$
	RR2	$\Lambda_1=\{ADA\}, \Lambda_2=\{AOA\},$ $\Lambda_3=\{AA\}, \Lambda_4=\{DD\},$ $\Lambda_5=\{DOD\}, \Lambda_6=\{DAD\}$	None	$\eta_4=\{O\}$	$\eta_1=\{AD\}, \eta_2=\{AO\},$ $\eta_3=\{A\}, \eta_5=\{D\},$ $\eta_6=\{DO\}, \eta_7=\{DA\}$	None	$\{\eta_1,\eta_2,\eta_3,\phi,\eta_5,\eta_6,\eta_7;OOC\}$
	S2		$\Psi_1=\{\pm A\},$ $\Psi_2=\{\pm D\},$ $\Psi_3=\{\pm OA\},$ $\Psi_4=\{\pm OD\}$			$\psi_1=\{\pm\},$ $\psi_2=\{\pm O\}$	$\{\eta_1,\eta_2,\eta_3,\phi,\eta_5,\eta_6,\eta_7,\psi_1,\psi_2;OOC\}$
	RR3	$\Lambda_1=\{AOA\}, \Lambda_2=\{AA\},$ $\Lambda_3=\{DD\}, \Lambda_4=\{DOD\}$	None	$\eta_3=\{O\}$	$\eta_1=\{AO\}, \eta_2=\{A\},$ $\eta_4=\{D\}, \eta_5=\{DO\}$	None	$\{\eta_1,\eta_2,\phi,\eta_4,\eta_5;OOC\}$
	S3		$\Psi_1=\{\pm A\},$ $\Psi_2=\{\pm D\},$ $\Psi_3=\{\pm OA\},$ $\Psi_4=\{\pm OD\}$			$\psi_1=\{\pm\},$ $\psi_2=\{\pm O\}$	$\{\eta_1,\eta_2,\phi,\eta_4,\eta_5,\psi_1,\psi_2;OOC\}$
	RR4	$\Lambda_1=\{ABA\}, \Lambda_2=\{AA\},$ $\Lambda_3=\{DD\}, \Lambda_4=\{DCD\}$	None	$\eta_3=\{B,C\}$	$\eta_1=\{AB\}, \eta_2=\{A\},$ $\eta_4=\{D\}, \eta_5=\{DC\}$	None	$\{\eta_1,\eta_2,\phi,\eta_4,\eta_5;OOC\}$
	S4		$\Psi_1=\{\pm A\},$ $\Psi_2=\{\pm D\},$ $\Psi_3=\{\pm BA\},$ $\Psi_4=\{\pm CD\}$			$\psi_1=\{\pm\},$ $\psi_2=\{\pm B\},$ $\psi_3=\{\pm C\}$	$\{\eta_1,\eta_2,\phi,\eta_4,\eta_5,\psi_1,\psi_2,\psi_3;OOC\}$

Table 4: TPMs of the *2-of-(H+1)* runs-rules and synthetic $\bar{X}$ charts when $H = 1$ and 2

$H = 1$

S1, RR1

	ϕ	η_2	OOC
ϕ	p_O	p_U	
η_2	p_O		p_U
OOC			1

S2, S3, S4, RR2, RR3, RR4

	η_1	ϕ	η_3	ψ_1	OOC
η_1		p_O	p_D		p_A
ϕ	p_A	p_O	p_D		
η_3	p_A	p_O			p_D
ψ_1		p_O			p_A+p_D
OOC					1

$H = 2$

S1, RR1

	ϕ	η_2	η_3	OOC
ϕ	p_O	p_U		
η_2			p_O	p_U
η_3	p_O			p_U
OOC				1

S2, RR2

	η_1	η_2	η_3	ϕ	η_5	η_6	η_7	ψ_1	ψ_2	OOC
η_1				p_O						$p_A + p_D$
η_2					p_O	p_D				p_A
η_3	p_D	p_O								p_A
ϕ			p_A	p_O	p_D					
η_5						p_O	p_A			p_D
η_6					p_A	p_O				p_D
η_7		p_O								$p_A + p_D$
ψ_1								p_O		$p_A + p_D$
ψ_2				p_O						$p_A + p_D$
OOC										1

S3, RR3

	η_1	η_2	ϕ	η_4	η_5	ψ_1	ψ_2	OOC
η_1			p_O	p_D				p_A
η_2	p_O			p_D				p_A
ϕ		p_A	p_O	p_D				
η_4		p_A			p_O			p_D
η_5		p_A	p_O					p_D
ψ_1						p_O	$p_A + p_D$	
ψ_2			p_O					$p_A + p_D$
OOC								1

S4, RR4

	η_1	η_2	ϕ	η_4	η_5	ψ_1	ψ_2	ψ_3	OOC
η_1			$p_B + p_C$	p_D					p_A
η_2	p_B		p_C	p_D					p_A
ϕ		p_A	$p_B + p_C$	p_D					
η_4		p_A	p_B		p_C				p_D
η_5		p_A	$p_B + p_C$						p_D
ψ_1							p_B	p_C	$p_A + p_D$
ψ_2			$p_B + p_C$	p_D					p_A
ψ_3		p_A	$p_B + p_C$						p_D
OOC									1

Similar to the *2-of-(H+1)* runs-rules schemes, the synthetic schemes have these compound patterns: $\Lambda = \Lambda_1 \cup \Lambda_2 \cup ... \cup \Lambda_\omega$; in addition, the synthetic schemes consists of compound patterns with a head-start feature. That is, let Ψ_r to be r^{th} simple pattern with the sequence of states starting with a head-start state, say $\Psi_r = \{\pm OOA\}$, where '$\pm$' indicates that a plotting statistic either falls above the *UCL* or below the *LCL*. Hence, we define Ψ as a compound pattern if it is the union of υ distinct simple patterns i.e. $\Psi = \Psi_1 \cup \Psi_2 \cup ... \cup \Psi_\upsilon$. Thus, for the synthetic schemes, W denote the waiting time for the first occurrence of either Λ or Ψ, i.e. the waiting time until the first occurrence of one of the patterns, $\Lambda_1,..., \Lambda_\omega, \Psi_1,..., \Psi_\upsilon$. If $\Psi_1 = \{\pm OOA\}$ then the corresponding transient sub-pattern is given by $\psi_1 = \{\pm OO\}$. Hence, $\eta_1,..., \eta_\tau$ and $\psi_1,..., \psi_\kappa$ are the distinct sub-patterns of the simple absorbing patterns $\Lambda_1,..., \Lambda_\omega$ and $\Psi_1,..., \Psi_\upsilon$, where $\tau \leq \omega$ and $\kappa < \upsilon$. In essence, we first define Λ and Ψ, and then extract the corresponding η's and ψ's as well as ϕ. Then using the Ω elements described in Table

3, we construct each of the corresponding TPMs in Table 4 when $H = 1$ and 2 for the synthetic and runs-rules (by removing the shaded elements or states) schemes, respectively.

In part from Tables 3 and 4, we deduced that: (i) by removing the head-start element (i.e. the shaded elements or states in Table 4) of the S2, S3 and S4 schemes yields the TPMs of the *2-of-(H+1)* RR2, RR3 and RR4 schemes; (ii) the TPM of the S1 scheme is the same as that of RR1 scheme; (iii) the dimension of the TPMs for any $H > 0$ are given by

$$M = \begin{cases} \tau & \text{for RR1, RR2, RR3, RR4} \\ \tau + \kappa & \text{for S1, S2, S3, S4} \end{cases} \tag{5}$$

where

$$\tau = \begin{cases} H + 1 & \text{for RR1, S1} \\ H^2 + H + 1 & \text{for RR2, S2} \\ 2H + 1 & \text{for RR3, RR4, S3, S4} \end{cases} \quad \text{and} \quad \kappa = \begin{cases} 0 & \text{for S1} \\ H & \text{for S2, S3} \\ 2H - 1 & \text{for S4.} \end{cases} \tag{6}$$

Note that to obtain TPMs with an obvious recursive pattern for any $H > 0$, we define the Ω as follows,

RR1 & S1: $\Omega = \{\eta_1 \equiv \phi, \eta_2, \dots, \eta_\tau; \text{OOC}\}$
RR2, RR3, RR4: $\Omega = \{\eta_1, \dots, \eta_{\frac{(\tau+1)}{2}-1}, \eta_{\frac{(\tau+1)}{2}} \equiv \phi, \eta_{\frac{(\tau+1)}{2}+1}, \dots, \eta_\tau; \text{OOC}\}$ (7)
S2, S3, S4: $\Omega = \{\eta_1, \dots, \eta_{\frac{(\tau+1)}{2}-1}, \eta_{\frac{(\tau+1)}{2}} \equiv \phi, \eta_{\frac{(\tau+1)}{2}+1}, \dots, \eta_\tau; \psi_1, \dots, \psi_\kappa; \text{OOC}\}.$

Therefore, from Equations (3) to (7) as well as Tables 3 and 4, it follows that for any $H > 0$, the TPMs of each of the schemes are as shown in Table 5, Panels (a) to (d).

Table 5: The general form of the TPMs of the synthetic and runs-rules $\bar{X}$ schemes

(a) S1 & RR1 schemes

	ϕ	η_2	η_3	η_4	η_5	$\cdots$	$\eta_{\tau-3}$	$\eta_{\tau-2}$	$\eta_{\tau-1}$	η_τ	OOC
ϕ	p_O	p_U				$\cdots$					
η_2			p_O			$\cdots$					p_U
η_3				p_O		$\cdots$					p_U
η_4					p_O	$\cdots$					p_U
$\vdots$						$\ddots$					$\vdots$
$\vdots$	$\vdots$	$\vdots$	$\vdots$	$\vdots$	$\vdots$	$\vdots$	$\ddots$				$\vdots$
$\eta_{\tau-3}$								p_O			p_U
$\eta_{\tau-2}$									p_O		p_U
$\eta_{\tau-1}$										p_O	p_U
η_τ	p_O										p_U
OOC											1

(b) S2 (removing the shaded elements yields RR2) scheme

For the S2 & RR2 schemes we need to define the following dummy variables to facilitate in easily writing the general form of the TPM:

$$a = H$$
$$b = H + (H - 1)$$
$$c = H + (H - 1) + (H - 2)$$

$$d = H + (H - 1) + (H - 2) + (H - 3)$$
$$\vdots$$
$$l = \frac{\tau + 1}{2}$$
$$\vdots$$
$$x = (\tau + 1) - c$$
$$y = (\tau + 1) - b$$
$$z = (\tau + 1) - a.$$

For convenience, let 'A', 'D' and 'O' denote 'p_A', 'p_D' and 'p_O', respectively.

	ϕ	OOC
η_1	O	A+D
η_2	O	A+D
η_3	O	A+D
$\vdots$	$\iddots$	$\vdots$
η_{a-2}	O	A+D
η_{a-1}	O	A+D
η_a	O D	A
η_{a+1}	O	A+D
η_{a+2}	O	A+D
η_{a+3}	O	A+D
$\vdots$	$\iddots$	$\vdots$
η_{b-1}	O	A+D
η_b	D O	A
η_{b+1}	O	A+D
$\vdots$	$\iddots$	$\vdots$
η_{c-1}	O	A+D
η_c	D O	A
η_{c+1}	O	A+D
$\vdots$	$\iddots$	$\vdots$
η_{l-7}	D O	A
η_{l-6}	O	A+D
η_{l-5}	O	A+D
η_{l-4}	D O	A
η_{l-3}	O	A+D
η_{l-2}	D O	A
η_{l-1}	D O	A
ϕ	**A O D**	
η_{l+1}	O A	D
η_{l+2}	O A	D
η_{l+3}	O	A+D
η_{l+4}	O A	D
η_{l+5}	O	A+D
η_{l+6}	O	A+D
η_{l+7}	O A	D
$\vdots$		$\vdots$
η_{x-1}	O	A+D
η_x	O A	D
η_{x+1}	O	A+D
$\vdots$		$\vdots$
η_{y-1}	O	A+D
η_y	O A	D
η_{y+1}	O	A+D
$\vdots$		$\vdots$
η_{z-1}	O	A+D
η_z	A O	D
η_{z+1}	O	A+D
η_{z+2}	O	A+D
$\vdots$		$\vdots$
$\eta_{\tau-2}$	O	A+D
$\eta_{\tau-1}$	O	A+D
η_τ	O	A+D
ψ_1	O	A+D
ψ_2	O	A+D
$\vdots$		$\vdots$

$\psi_{\kappa-1}$						O	A+D
ψ_κ				O			A+D
OOC							1

(c) S3 (removing the shaded elements yields RR3) scheme

	η_1	η_2	$\cdots$	η_{l-4}	η_{l-3}	η_{l-2}	η_{l-1}	ϕ	η_{l+1}	η_{l+2}	η_{l+3}	η_{l+4}	$\cdots$	$\eta_{\tau-2}$	$\eta_{\tau-1}$	η_τ	ψ_1	ψ_2	ψ_3	ψ_4	$\cdots$	$\psi_{\kappa-2}$	$\psi_{\kappa-1}$	ψ_κ	OOC
η_1								p_O	p_D																p_A
η_2	p_O								p_D																p_A
η_3		p_O							p_D																p_A
$\vdots$			$\ddots$						$\vdots$																$\vdots$
η_{l-3}				p_O					p_D																p_A
η_{l-2}					p_O				p_D																p_A
η_{l-1}						p_O			p_D																p_A
ϕ							p_A	p_O	p_D																
η_{l+1}								p_A		p_O															p_D
η_{l+2}								p_A			p_O														p_D
η_{l+3}								p_A				p_O													p_D
$\vdots$								p_A					$\ddots$												$\vdots$
$\eta_{\tau-3}$								p_A						p_O											p_D
$\eta_{\tau-2}$								p_A							p_O										p_D
$\eta_{\tau-1}$								p_A								p_O									p_D
η_τ								p_A	p_O																p_D
ψ_1																	p_O								p_A+p_D
ψ_2																		p_O							p_A+p_D
ψ_3																			p_O						p_A+p_D
$\vdots$																				$\ddots$					$\vdots$
$\psi_{\kappa-3}$																						p_O			p_A+p_D
$\psi_{\kappa-2}$																							p_O		p_A+p_D
$\psi_{\kappa-1}$																								p_O	p_A+p_D
ψ_κ								p_O																	p_A+p_D
OOC																									1

(d) S4 (removing the shaded elements yields RR4) scheme

	η_1	η_2	$\cdots$	η_{l-3}	η_{l-2}	η_{l-1}	ϕ	η_{l+1}	η_{l+2}	η_{l+3}	$\cdots$	$\eta_{\tau-2}$	$\eta_{\tau-1}$	η_τ	ψ_1	ψ_2	ψ_3	ψ_4	ψ_5	$\cdots$	$\psi_{\kappa-3}$	$\psi_{\kappa-2}$	$\psi_{\kappa-1}$	ψ_κ	OOC
η_1							p_B+p_C	p_D																	p_A
η_2	p_B						p_C	p_D																	p_A
η_3		p_B					p_C	p_D																	p_A
$\vdots$			$\ddots$				$\vdots$	$\vdots$																	$\vdots$
η_{l-2}				p_B			p_C	p_D																	p_A
η_{l-1}					p_B		p_C	p_D																	p_A
ϕ						p_A	p_B+p_C	p_D																	
η_{l+1}						p_A	p_B			p_C															p_D
η_{l+2}						p_A	p_B				p_C														p_D
$\vdots$							$\vdots$					$\ddots$													$\vdots$
$\eta_{\tau-3}$						p_A	p_B						p_C												p_D
$\eta_{\tau-2}$						p_A	p_B							p_C											p_D
$\eta_{\tau-1}$						p_A	p_B								p_C										p_D
η_τ						p_A	p_B+p_C																		p_D
ψ_1																p_B	p_C								p_A+p_D
ψ_2							p_C	p_D										p_B							p_A
ψ_3						p_A	p_B												p_C						p_D
$\vdots$							$\vdots$													$\ddots$					$\vdots$
$\psi_{\kappa-5}$							p_C	p_D													p_B				p_A
$\psi_{\kappa-4}$						p_A	p_B															p_C			p_D
$\psi_{\kappa-3}$							p_C	p_D															p_B		p_A
$\psi_{\kappa-2}$						p_A	p_B																	p_C	p_D
$\psi_{\kappa-1}$							p_B+p_C	p_D																	p_A
ψ_κ						p_A	p_B+p_C																		p_D
OOC																									1

3. Average run-length vectors

Here, we formulate the $\boldsymbol{ARL}_{(M\times1)}$ vectors in Equation (1) for each of the schemes. This procedure is conducted recursively and, based on the patterns of these expressions as H increases, we use mathematical or complete induction to formulate the general form of the *ARL* vectors.

Using Equation (1) and the TPM in Table 5, Panel (a), the *ARL* vector of the S1 and RR1 is given by Equation (8).

$$\boldsymbol{ARL}(\delta) = (\mathbf{I} - \mathbf{Q}(\delta))^{-1}\mathbf{1} = \begin{pmatrix} \phi = \varsigma_1(\delta) \\ \varsigma_2(\delta) \\ \varsigma_3(\delta) \\ \varsigma_4(\delta) \\ \vdots \\ \varsigma_{H-2}(\delta) \\ \varsigma_{H-1}(\delta) \\ \varsigma_H(\delta) \\ \varsigma_{H+1}(\delta) \end{pmatrix} = \frac{1}{1 - p_O - p_O^H + p_O^{H+1}} \begin{pmatrix} 2 - p_O^H \\ 1 \\ 1 + p_O^{H-1} - p_O^H \\ 1 + p_O^{H-2} - p_O^H \\ \vdots \\ 1 + p_O^4 - p_O^H \\ 1 + p_O^3 - p_O^H \\ 1 + p_O^2 - p_O^H \\ 1 + p_O - p_O^H \end{pmatrix}. \tag{8}$$

While the TPM of the S1 scheme is exactly equivalent to that of the RR1 scheme, this is not the case for the other schemes, that is, to obtain the TPMs of the RR2, RR3 and RR4 schemes from the TPMs of the S2, S3, S4 schemes, we need to remove the components that correspond to the head-start feature. Consequently, to derive the $\boldsymbol{ARL}_{1\times\tau}^{\text{RR}}$ (*ARL* vector of runs-rules (RR) scheme) from the $\boldsymbol{ARL}_{1\times(\tau+\kappa)}^{\text{synth}}$ (*ARL* vector of synthetic scheme), we need to remove the $\boldsymbol{ARL}_{1\times\kappa}^{\text{HS}}$ (the components corresponding to the head-start (HS) feature), that is, assume that '//' denotes the vertical concatenation operator, then it is easy to see that:

$$\boldsymbol{ARL}_{1\times(\tau+\kappa)}^{\text{synth}} \equiv \boldsymbol{ARL}_{1\times\tau}^{\text{RR}} // \boldsymbol{ARL}_{1\times\kappa}^{\text{HS}}. \tag{9}$$

Note that great attempts to obtain the closed-form expressions of the S2 and RR2 schemes were made; however, we concluded that these are impossible as we were unable to obtain any apparent recursive relationship. Next, for the S3 and RR3 schemes, $\mathfrak{D}(\delta) = 1 - p_O - p_A p_O^H - p_D p_O^H - p_A p_D \sum_{i=0}^{2H-1} p_O^i$ and $\mathbf{Q}_{(3H+1)\times(3H+1)}$ is given in Table 5, Panel (c) and then using Equations (1) and (9), the $\boldsymbol{ARL}_{1\times(\tau+\kappa)}^{\text{synth}} \equiv \boldsymbol{ARL}_{1\times\tau}^{\text{RR}} // \boldsymbol{ARL}_{1\times\kappa}^{\text{HS}} = \left(\mathbf{I} - \mathbf{Q}_{(3H+1)\times(3H+1)}\right)^{-1}\mathbf{1}$ yields Equation (10).

$$\phi = \begin{pmatrix} \varsigma_1(\delta) \\ \varsigma_2(\delta) \\ \vdots \\ \varsigma_{H-3}(\delta) \\ \varsigma_{H-2}(\delta) \\ \varsigma_{H-1}(\delta) \\ \varsigma_H(\delta) \\ \varsigma_{H+1}(\delta) \\ \varsigma_{H+2}(\delta) \\ \varsigma_{H+3}(\delta) \\ \varsigma_{H+4}(\delta) \\ \varsigma_{H+5}(\delta) \\ \vdots \\ \varsigma_{2H}(\delta) \\ \varsigma_{2H+1}(\delta) \\ \psi_1 = \varsigma_{2H+2}(\delta) \\ \varsigma_{2H+3}(\delta) \\ \varsigma_{2H+4}(\delta) \\ \varsigma_{2H+5}(\delta) \\ \vdots \\ \varsigma_{3H}(\delta) \\ \varsigma_{3H+1}(\delta) \end{pmatrix} = \frac{1}{\mathfrak{D}(\delta)} \begin{pmatrix} \left(1 + p_A p_O \sum_{i=0}^{H-2} p_O^i\right)\left(1 + p_D \sum_{i=0}^{H-1} p_O^i\right) \\ \left(1 + p_A p_O^2 \sum_{i=0}^{H-3} p_O^i\right)\left(1 + p_D \sum_{i=0}^{H-1} p_O^i\right) \\ \vdots \\ \left(1 + p_A p_O^{H-3} \sum_{i=0}^{2} p_O^i\right)\left(1 + p_D \sum_{i=0}^{H-1} p_O^i\right) \\ \left(1 + p_A p_O^{H-2} \sum_{i=0}^{1} p_O^i\right)\left(1 + p_D \sum_{i=0}^{H-1} p_O^i\right) \\ (1 + p_A p_O^{H-1})\left(1 + p_D \sum_{i=0}^{H-1} p_O^i\right) \\ 1 + p_D \sum_{i=0}^{H-1} p_O^i \\ \left(1 + p_A \sum_{i=0}^{H-1} p_O^i\right)\left(1 + p_D \sum_{i=0}^{H-1} p_O^i\right) \\ 1 + p_A \sum_{i=0}^{H-1} p_O^i \\ (1 + p_D p_O^{H-1})\left(1 + p_A \sum_{i=0}^{H-1} p_O^i\right) \\ \left(1 + p_D p_O^{H-2} \sum_{i=0}^{1} p_O^i\right)\left(1 + p_A \sum_{i=0}^{H-1} p_O^i\right) \\ \left(1 + p_D p_O^{H-3} \sum_{i=0}^{2} p_O^i\right)\left(1 + p_A \sum_{i=0}^{H-1} p_O^i\right) \\ \vdots \\ \left(1 + p_D p_O^2 \sum_{i=0}^{H-3} p_O^i\right)\left(1 + p_A \sum_{i=0}^{H-1} p_O^i\right) \\ \left(1 + p_D p_O \sum_{i=0}^{H-2} p_O^i\right)\left(1 + p_A \sum_{i=0}^{H-1} p_O^i\right) \\ 1 - p_A p_D \left(\sum_{i=0}^{H-1} p_O^i\right)^2 \\ 1 + p_A p_O^{H-1} + p_D p_O^{H-1} - p_A p_D \left[1 + p_O\left(2 + p_O\left(3 + p_O\left(\ldots\left((H-2) + p_O\left((H-1) + p_O\left((H-2) + p_O\left(\ldots(3 + p_O(2 + p_O - p_O^3))\ldots\right)\right)\right)\right)\ldots\right)\right)\right)\right] \\ 1 + p_A p_O^{H-2} \sum_{i=0}^{1} p_O^i + p_D p_O^{H-2} \sum_{i=0}^{1} p_O^i + p_A p_D \left(\sum_{i=H-2}^{H-1} p_O^i - \sum_{i=0}^{H-3} p_O^i\right)\left(\sum_{i=0}^{H-1} p_O^i\right) \\ 1 + p_A p_O^{H-3} \sum_{i=0}^{2} p_O^i + p_D p_O^{H-3} \sum_{i=0}^{2} p_O^i + p_A p_D \left(\sum_{i=H-3}^{H-1} p_O^i - \sum_{i=0}^{H-4} p_O^i\right)\left(\sum_{i=0}^{H-1} p_O^i\right) \\ \vdots \\ 1 + p_A p_O^2 \sum_{i=0}^{H-3} p_O^i + p_D p_O^2 \sum_{i=0}^{H-3} p_O^i + p_A p_D \left(\sum_{i=2}^{H-1} p_O^i - \sum_{i=0}^{1} p_O^i\right)\left(\sum_{i=0}^{H-1} p_O^i\right) \\ 1 + p_A p_O \sum_{i=0}^{H-2} p_O^i + p_D p_O \sum_{i=0}^{H-2} p_O^i + p_A p_D \left(\sum_{i=1}^{H-1} p_O^i - \sum_{i=0}^{0} p_O^i\right)\left(\sum_{i=0}^{H-1} p_O^i\right) \end{pmatrix}.$$

$$\ldots\ldots\ldots\ldots(10)$$

For the S4 and RR4 schemes, using Equations (1) and (9), the *ARL* vector is given by Equation (11), where $\mathbf{Q}_{(4H)\times(4H)}$ is given in Table 5, Panel (d) and

$$\mathfrak{D}(\delta) = 1 - p_A\left(p_C + p_D + p_D p_C \sum_{i=0}^{H-1} p_C^i\right) - p_B\left(1 + p_D \sum_{i=0}^{H-1} p_C^i\right) - p_C - p_A p_B^H\left(1 + p_D \sum_{i=0}^{H-1} p_C^i\right) - p_D p_C^H - p_A \sum_{j=1}^{H-1} p_B^j\left(p_C + p_D + p_D p_C \sum_{i=0}^{H-1} p_C^i\right).$$

$$ARL_{1\times(\tau+\kappa)}^{\text{synth}} \equiv ARL_{1\times\tau}^{\text{RR}}//ARL_{1\times\kappa}^{\text{HS}} = \left(I - Q_{(4H)\times(4H)}\right)^{-1} 1 = \begin{pmatrix} \varsigma_1(\delta) \\ \varsigma_2(\delta) \\ \vdots \\ \varsigma_{H-3}(\delta) \\ \varsigma_{H-2}(\delta) \\ \varsigma_{H-1}(\delta) \\ \varsigma_H(\delta) \\ \phi = \varsigma_{H+1}(\delta) \\ \varsigma_{H+2}(\delta) \\ \varsigma_{H+3}(\delta) \\ \varsigma_{H+4}(\delta) \\ \varsigma_{H+5}(\delta) \\ \vdots \\ \varsigma_{2H}(\delta) \\ \varsigma_{2H+1}(\delta) \\ \psi_1 = \varsigma_{2H+2}(\delta) \\ \varsigma_{2H+3}(\delta) \\ \varsigma_{2H+4}(\delta) \\ \varsigma_{2H+5}(\delta) \\ \varsigma_{2H+6}(\delta) \\ \varsigma_{2H+7}(\delta) \\ \varsigma_{2H+8}(\delta) \\ \vdots \\ \varsigma_{4H-3}(\delta) \\ \varsigma_{4H-2}(\delta) \\ \varsigma_{4H-1}(\delta) \\ \varsigma_{4H}(\delta) \end{pmatrix} = \frac{1}{\mathfrak{D}(\delta)} \begin{pmatrix} \left(1 + p_A p_B \sum_{i=0}^{H-2} p_B^i\right)\left(1 + p_D \sum_{i=0}^{H-1} p_C^i\right) \\ \left(1 + p_A p_B^2 \sum_{i=0}^{H-3} p_B^i\right)\left(1 + p_D \sum_{i=0}^{H-1} p_C^i\right) \\ \vdots \\ \left(1 + p_A p_B^{H-3} \sum_{i=0}^{2} p_B^i\right)\left(1 + p_D \sum_{i=0}^{H-1} p_C^i\right) \\ \left(1 + p_A p_B^{H-2} \sum_{i=0}^{1} p_B^i\right)\left(1 + p_D \sum_{i=0}^{H-1} p_C^i\right) \\ (1 + p_A p_B^{H-1})\left(1 + p_D \sum_{i=0}^{H-1} p_C^i\right) \\ 1 + p_D \sum_{i=0}^{H-1} p_C^i \\ \left(1 + p_A \sum_{i=0}^{H-1} p_B^i\right)\left(1 + p_D \sum_{i=0}^{H-1} p_C^i\right) \\ 1 + p_A \sum_{i=0}^{H-1} p_B^i \\ (1 + p_D p_C^{H-1})\left(1 + p_A \sum_{i=0}^{H-1} p_B^i\right) \\ \left(1 + p_D p_C^{H-2} \sum_{i=0}^{1} p_C^i\right)\left(1 + p_A \sum_{i=0}^{H-1} p_B^i\right) \\ \left(1 + p_D p_C^{H-3} \sum_{i=0}^{2} p_C^i\right)\left(1 + p_A \sum_{i=0}^{H-1} p_B^i\right) \\ \vdots \\ \left(1 + p_D p_C^2 \sum_{i=0}^{H-3} p_C^i\right)\left(1 + p_A \sum_{i=0}^{H-1} p_B^i\right) \\ \left(1 + p_D p_C \sum_{i=0}^{H-2} p_C^i\right)\left(1 + p_A \sum_{i=0}^{H-1} p_B^i\right) \\ 1 - p_A p_D \left(\sum_{i=0}^{H-1} p_B^i\right)\left(\sum_{i=0}^{H-1} p_C^i\right) \\ (1 + p_A p_B^{H-1})\left(1 + p_D \sum_{i=0}^{H-1} p_C^i\right) \\ (1 + p_D p_C^{H-1})\left(1 + p_A \sum_{i=0}^{H-1} p_B^i\right) \\ \left(1 + p_A p_B^{H-2} \sum_{i=0}^{1} p_B^i\right)\left(1 + p_D \sum_{i=0}^{H-1} p_C^i\right) \\ \left(1 + p_D p_C^{H-2} \sum_{i=0}^{1} p_C^i\right)\left(1 + p_A \sum_{i=0}^{H-1} p_B^i\right) \\ \left(1 + p_A p_B^{H-3} \sum_{i=0}^{2} p_B^i\right)\left(1 + p_D \sum_{i=0}^{H-1} p_C^i\right) \\ \left(1 + p_D p_C^{H-3} \sum_{i=0}^{2} p_C^i\right)\left(1 + p_A \sum_{i=0}^{H-1} p_B^i\right) \\ \vdots \\ \left(1 + p_A p_B^2 \sum_{i=0}^{H-3} p_B^i\right)\left(1 + p_D \sum_{i=0}^{H-1} p_C^i\right) \\ \left(1 + p_D p_C^2 \sum_{i=0}^{H-3} p_C^i\right)\left(1 + p_A \sum_{i=0}^{H-1} p_B^i\right) \\ \left(1 + p_A p_B \sum_{i=0}^{H-2} p_B^i\right)\left(1 + p_D \sum_{i=0}^{H-1} p_C^i\right) \\ \left(1 + p_D p_C \sum_{i=0}^{H-2} p_C^i\right)\left(1 + p_A \sum_{i=0}^{H-1} p_B^i\right) \end{pmatrix}. \tag{11}$$

4. Synthetic chart's run-length expressions

In this section, we provide the initial probability vectors and formulate the *ZSARL* expressions of the synthetic schemes in Table 1.

4.1 Initial probabilities vectors

The $\mathbf{q}_{(1\times M)}$ has a value of one in the component associated with the state in which the chart begins and each of the other components are zero. For the synthetic charts, the 'η_2' denotes the initial state of the S1 scheme and 'ψ_1' denotes the initial state of the S2, S3 and S4 schemes – see Section 2. Therefore, given the state space in Equation (7), the initial state probability vectors, for each of the schemes, are given by

$$S1: \mathbf{q}_{(1\times M)} = (0\ 1\ 0\ \dots\ 0) \text{ i.e. the } 2^{\text{nd}} \text{ one,}$$

$$S2, S3, S4: \mathbf{q}_{(1\times M)} = (0\ 0\ \dots 0\ 1_{(\tau+1)}\ \dots 0) \text{ i.e. the } (\tau+1)^{\text{th}} \text{ one.}$$

$$(12)$$

4.2 Average run-length expressions

The *ZSARL*s are the product of the $\mathbf{q}$'s (in Equation (12)) and the *ARL*s (in Section 3), that is, $ZSARL = \mathbf{q} \cdot \boldsymbol{ARL}(\delta)$ yields the closed-form expressions as given below:

S1: $\dfrac{1}{1 - p_O - p_O^H + p_O^{H+1}},$

S2: Does not exist,

S3: $\dfrac{1 - p_A p_D \left(\sum_{i=0}^{H-1} p_O^i\right)^2}{1 - p_O - p_A p_O^H - p_D p_O^H - p_A p_D \sum_{i=0}^{2H-1} p_O^i},$

S4: $\dfrac{1 - p_A p_D \left(\sum_{i=0}^{H-1} p_B^i\right)\left(\sum_{i=0}^{H-1} p_C^i\right)}{1 - p_A\left(p_C + p_D + p_D p_C \sum_{i=0}^{H-1} p_C^i\right) - p_B\left(1 + p_D \sum_{i=0}^{H-1} p_C^i\right) - p_C - p_A p_B^H\left(1 + p_D \sum_{i=0}^{H-1} p_C^i\right) - p_D p_C^H - p_A \sum_{j=1}^{H-1} p_B^j\left(p_C + p_D + p_D p_C \sum_{i=0}^{H-1} p_C^i\right)}.$

To this point, only the closed-form expression of the S1 scheme had existed, see Wu and Spedding (2000) – note though, while theirs is exactly equivalent to the one given above, it is derived and written in a different manner.

5. Runs-rules chart's run-length expressions

In this section, we provide the initial probability vectors and formulate the *ZSARL* expressions of the runs-rules schemes in Table 2.

5.1 Initial probabilities vectors

The $\mathbf{q}_{(1\times\tau)}$ has a value of one in the component associated with the state in which the chart begins and each of the other components are zero. The 'ϕ' state denotes the initial state of all the four runs-rules schemes and from the state space in Equation (7), the initial state probability vectors for each of the schemes are given by

$$\text{RR1: } \mathbf{q}_{(1\times\tau)} = (1\ 0\ 0\ \dots\ 0) \text{ i.e. the } 1^{\text{st}} \text{ one,}$$

$$\text{RR2, RR3, RR4: } \mathbf{q}_{(1\times\tau)} = (0\ 0\ \dots\ 1_{\frac{(\tau+1)}{2}}\ \dots 0\ 0) \text{ i.e. the } \left(\frac{\tau+1}{2}\right)^{\text{th}} \text{ one.}$$

(13)

5.2 Average run-length expressions

The *ZSARL*s are the product of the $\mathbf{q}$'s (in Equation (13)) and the **ARL**s (in Section 3 and keeping in mind Equation (9)), that is, $ZSARL = \mathbf{q} \cdot \mathbf{ARL}(\delta)$ yields the closed-form expressions given by:

RR1: $\dfrac{2 - p_O^H}{1 - p_O - p_O^H + p_O^{H+1}}$,

RR2: Does not exist,

RR3: $\dfrac{\left(1 + p_A \sum_{i=0}^{H-1} p_O^i\right)\left(1 + p_D \sum_{i=0}^{H-1} p_O^i\right)}{1 - p_O - p_A p_O^H - p_D p_O^H - p_A p_D \sum_{i=0}^{2H-1} p_O^i}$,

RR4: $\dfrac{\left(1 + p_A \sum_{i=0}^{H-1} p_B^i\right)\left(1 + p_D \sum_{i=0}^{H-1} p_C^i\right)}{1 - p_A\left(p_C + p_D + p_D p_C \sum_{i=0}^{H-1} p_C^i\right) - p_B\left(1 + p_D \sum_{i=0}^{H-1} p_C^i\right) - p_C - p_A p_B^H\left(1 + p_D \sum_{i=0}^{H-1} p_C^i\right) - p_D p_C^H - p_A \sum_{j=1}^{H-1} p_B^j\left(p_C + p_D + p_D p_C \sum_{i=0}^{H-1} p_C^i\right)}$.

To the best of our knowledge, none of these simple closed-form expressions currently exist in the literature.

6. Overall run-length performance measures

The overall performance measures (i.e. zero-state *EQL*, *ARARL* and *PCI*) for each of the synthetic and runs-rules schemes that were used by Shongwe and Graham (2018) as empirical evaluation tools can be computed using the zero-state *EWRL* expressions presented in Table 6, which, for future research purpose, we intend to use as the design optimization functions.

Moreover, Shongwe and Graham (2018) only considered the case where δ follows a uniform distribution and parameters are specified. We intend to investigate the effect of: (i) the use of a variety of distributions of δ; (ii) parameter estimation; and (iii) the use of some other run-length metric instead of Equations (1) and (2), for instance, the percentile or median run-length.

Table 6: The zero-state *EWRL* expressions of the *2-of-(H+1)* runs-rules and synthetic $\bar{X}$ charts

RR1:	$\displaystyle \int_{\delta_{min}}^{\delta_{max}} w(\delta) \times \left(\frac{2 - p_O^H}{1 - p_O - p_O^H + p_O^{H+1}} \right) \times f(\delta)\, d\delta$
RR2:	$\displaystyle \int_{\delta_{min}}^{\delta_{max}} w(\delta) \times \left(\mathbf{q}_{(1\times(H^2+H+1))} \cdot \left(\mathbf{I} - \mathbf{Q}_{((H^2+H+1)\times(H^2+H+1))} \right)^{-1} \cdot \mathbf{1} \right) \times f(\delta)\, d\delta$
RR3:	$\displaystyle \int_{\delta_{min}}^{\delta_{max}} w(\delta) \times \left(\frac{\left(1 + p_A \sum_{i=0}^{H-1} p_O^i\right)\left(1 + p_D \sum_{i=0}^{H-1} p_O^i\right)}{1 - p_O - p_A p_O^H - p_D p_O^H - p_A p_D \sum_{i=0}^{2H-1} p_O^i} \right) \times f(\delta)\, d\delta$
RR4:	$\displaystyle \int_{\delta_{min}}^{\delta_{max}} w(\delta) \times \left(\frac{\left(1 + p_A \sum_{i=0}^{H-1} p_B^i\right)\left(1 + p_D \sum_{i=0}^{H-1} p_C^i\right)}{1 - p_A\left(p_C + p_D + p_D p_C \sum_{i=0}^{H-1} p_C^i\right) - p_B\left(1 + p_D \sum_{i=0}^{H-1} p_C^i\right) - p_C - p_A p_B^H\left(1 + p_D \sum_{i=0}^{H-1} p_C^i\right) - p_D p_C^H - p_A \sum_{j=1}^{H-1} p_B^j\left(p_C + p_D + p_D p_C \sum_{i=0}^{H-1} p_C^i\right)} \right) \times f(\delta)\, d\delta$
S1:	$\displaystyle \int_{\delta_{min}}^{\delta_{max}} w(\delta) \times \left(\frac{1}{1 - p_O - p_O^H + p_O^{H+1}} \right) \times f(\delta)\, d\delta$
S2:	$\displaystyle \int_{\delta_{min}}^{\delta_{max}} w(\delta) \times \left(\mathbf{q}_{(1\times(H^2+2H+1))} \cdot \left(\mathbf{I} - \mathbf{Q}_{((H^2+2H+1)\times(H^2+2H+1))} \right)^{-1} \cdot \mathbf{1} \right) \times f(\delta)\, d\delta$
S3:	$\displaystyle \int_{\delta_{min}}^{\delta_{max}} w(\delta) \times \left(\frac{1 - p_A p_D \left(\sum_{i=0}^{H-1} p_O^i\right)^2}{1 - p_O - p_A p_O^H - p_D p_O^H - p_A p_D \sum_{i=0}^{2H-1} p_O^i} \right) \times f(\delta)\, d\delta$
S4:	$\displaystyle \int_{\delta_{min}}^{\delta_{max}} w(\delta) \times \left(\frac{1 - p_A p_D \left(\sum_{i=0}^{H-1} p_B^i\right)\left(\sum_{i=0}^{H-1} p_C^i\right)}{1 - p_A\left(p_C + p_D + p_D p_C \sum_{i=0}^{H-1} p_C^i\right) - p_B\left(1 + p_D \sum_{i=0}^{H-1} p_C^i\right) - p_C - p_A p_B^H\left(1 + p_D \sum_{i=0}^{H-1} p_C^i\right) - p_D p_C^H - p_A \sum_{j=1}^{H-1} p_B^j\left(p_C + p_D + p_D p_C \sum_{i=0}^{H-1} p_C^i\right)} \right) \times f(\delta)\, d\delta$

7. A comment on zero-state vs. steady-state mode

As mentioned earlier, in this paper (i.e. Part I), we only focus on the zero-state mode. The steady-state mode is reported in a separate paper (i.e. Part II). It is interesting to note that, in the literature, it seems that the trend is that researchers do not report on both the steady-state mode and the zero-mode under the same research (i.e. in the same paper). It seems that only one mode is selected upfront and investigated. For example, the zero-state mode of the Poisson GWMA chart is investigated in Chiu and Sheu (2008), whereas the steady-state mode is only investigated seven years later in Chiu and Lu (2015). And it is a continuing trend where authors have a publication on one mode and, only later, publish the results on the other mode. We strongly advise against this, since not only is it important to consider both modes, but it is of great importance to compare the zero-state performance and the steady-state performance of the proposed chart with that of competing charts. The reader is referred to the paper by Shongwe and Graham (2018) where both states are considered for all types of Shewhart synthetic and runs-rules $\bar{X}$ schemes. It is of great importance to consider both modes, since both can realize in practice; the zero-state mode is the appropriate measure if the process shifts at the start of the process and the steady-state mode is the appropriate measure the shift occurs some random time in the future. There is some indication that current publications are considering both modes; see Haq and Khoo (2016) for another example where both states were reported for their newly proposed auxiliary-information-based synthetic chart. However, unfortunately, other recent publications only focus on one mode without even making any mention of the other mode; see for example Polunchenko (2016) where only the zero-state is mentioned.

8. Concluding remarks

Since there is very little research on theoretical work of synthetic and runs-rules schemes and the fact that some authors are not familiar with Markov chain and / or Monte Carlo simulation, the zero-state expressions derived here will ease the implementation as well as further academic research in the area of Shewhart-type synthetic and / or runs-rules $\bar{X}$ monitoring schemes.

Although we were unable to compute the closed-form expressions for the S2 and RR2 schemes, the *ZSARL* of the S2 and RR2 schemes can be directly computed for any *H* using some software (e.g. SAS®, Matlab®, Mathematica®, etc.) by using the standard Markov chain equation. Moreover, the zero-state *ARL*s, *EQL*s, *PCI*s and *ARARL*s of the S2 and RR2 schemes as well as those of the S3 and RR3 schemes are approximately equal as δ varies, however, with those of the S3 and RR3 schemes having zero-state *ARL*s, *EQL*s, *PCI*s and *ARARL*s that are uniformly smaller than those of the S2 and RR2 schemes, respectively. Moreover, the S3 and RR3 schemes are much easier to evaluate as compared to the S2 and RR2 schemes, respectively. Thus, it follows that we need to re-think about the use of the S2 and RR2 schemes.

9. Future recommendations

1. The results in this article are based on the assumption of i.i.d. normally distributed observations and as part of future research work; we intend to extend this similar investigation for other monitoring schemes as well as for nonparametric schemes.

2. Researchers are urged to consider both zero-state and steady-state modes when designing a new control chart, since both can occur in practice.

3. The effectiveness of traditional performance measures should be revisited and this is currently under investigation.

4. Finally, it is worth mentioning that Shewhart synthetic chart (or more specifically, the S1 scheme of Wu and Spedding (2000)) has received a lot of criticism with most noticeably by Knoth (2016). While Knoth (2016) did prove that the EWMA and CUSUM schemes have a better performance than the Shewhart S1 scheme, we believe that the manner in which the author conducted his investigation was unfair as the EWMA-type and CUSUM-type schemes are generally known to have a better performance than many vastly sensitized Shewhart-type schemes. Moreover, we believe that the author's argument would have been more convincing if he had shown that, say, the EWMA-type or CUSUM-type S1 scheme (see Scariano and Calzada (2009) and Haq et al. (2013)) has no improvement over the standard EWMA or CUSUM monitoring schemes, of which, according to the two latter articles actually does yield an improvement. In the case of Shewhart synthetic charts, Knoth (2016) only considered a single type of synthetic chart (termed here as S1), however, from Table 1, it is apparent that there are four types of these and it is empirically shown in Shongwe and Graham (2018) that the other three synthetic-type schemes have a better performance than the one considered in Knoth (2016). Based on this argument, it is our opinion that before we accept the recommendations in Knoth (2016) to abandon the synthetic design, that we should re-visit the investigations that were conducted in the following articles: Scariano and Calzada (2009), Haq et al. (2013), Shongwe and Graham (2018) – as there seem to be some contradictions with certain deductions given in Knoth (2016). Note though the authors of this paper are also in the process of investigating the performance of all (Shewhart-, EWMA- and CUSUM-) types of synthetic schemes.

References

Antzoulakos, D.L. & Rakitzis, A.C. (2008). The modified *r* out of *m* control chart. *Communications in Statistics - Simulation and Computation*, 37(2), 396-408.

Benneyan, J.C., Lloyd, R.C. & Plsek, P.E. (2003). Statistical process control as a tool for research and healthcare improvement. *Quality, Safety and Health Care*, 12(6), 458-464.

Bourke, P. D. (1991). Detecting a shift in fraction nonconforming using run-length control charts with 100% inspection. *Journal of Quality Technology*, 23(3), 225-238.

Chiu, W.-C. & Lu, S.-L. (2015). On the steady-state performance of the Poisson double GWMA control chart. *Quality Technology & Quantitative Management*, 12(2), 195-208.

Chiu, W.-C. & Sheu, S.-H. (2008). Fast initial response features for Poisson GWMA control charts. *Communications in Statistics – Simulation and Computation*, 37(7), 1422-1439.

Davis, R.B. & Woodall, W.H (2002). Evaluating and improving the synthetic control chart. *Journal of Quality Technology*, 34(2), 200-208.

Derman, C. & Ross, S.M. (1997). *Statistical Aspects of Quality Control*. Academic Press, San Diego, CA.

Fu, J.C. & Lou, W.Y.W. (2003). *Distribution Theory of Runs and Patterns and Its Applications: A Finite Markov Chain Imbedding Approach.* Singapore: World Scientific Publishing.

Haq,. A. & Khoo, M.B.C. (2016). A new synthetic control chart for monitoring process mean using auxiliary information. *Journal of Statistical Computation and Simulation*, 86(15), 3068-3092.

Haq, A., Brown, J. & Moltchanova, E. (2013). New synthetic EWMA and synthetic CUSUM control charts for monitoring the process mean. *Quality and Reliability Engineering International*, 32(1), 269-290.

Huh, I. (2014). Optimal monitoring methods for univariate and multivariate EWMA control charts. *Published PhD thesis*, School of Graduate Studies, McMaster University, Canada.

Khoo, M.B.C. (2013). Recent developments on synthetic control charts. Proceedings of the *2013 IEEE Symposium on Business, Engineering and Industrial Applications* (*ISBEIA*), 460-465.

Klein, M. (2000). Two alternatives to the Shewhart $\bar{X}$ control chart. *Journal of Quality Technology*, 32(4), 427-431.

Knoth, S. (2016). The case against the use of synthetic control charts. *Journal of Quality Technology*, 48(2), 178-195.

Koutras, M.V., Bersimis, S. & Maravelakis, P.E. (2007). Statistical process control using Shewhart control charts with supplementary runs rules. *Methodology and Computing in Applied Probability*, 9(2), 207-224.

Machado, M.A.G. & Costa A.F.B. (2014). Some comments regarding the synthetic chart. *Communications in Statistics - Theory and Methods*, 43 (14), 2897-2906.

Machado, M.A.G. & Costa A.F.B. (2014). A side-sensitive synthetic chart combined with an $\bar{X}$ chart. *International Journal of Production Research*, 52 (11), 3404-3416.

Montgomery, D.C. (2013). *Statistical Quality Control: A Modern Introduction* (7th edn). John Wiley & Sons, Singapore Pte. Ltd.

Polunchenko (2016). A note on efficient performance evaluation of the cumulative sum chart and the sequential probability ratio test. *Applied Stochastic Models in Business and Industry*, 32(5), 565-573.

Qiu, P. (2014). Introduction to Statistical Process Control. Taylor & Francis Group.

Reynolds Jr., M.R. & Lou, J. (2010). An evaluation of a GLR control chart for monitoring the process mean. *Journal of Quality Technology*, 42 (3), 287-310.

Ryu, J-H., Wan, H. & Kim, S. (2010). Optimal design of a CUSUM chart for a mean shift of unknown size. *Journal of Quality Technology*, 42 (3), 311-326.

Scariano, S.M. & Calzada, M.E. (2009). The generalized synthetic chart. *Sequential Analysis*, 28(1), 54-68.

Shongwe, S.C. & Graham, M.A. (2018). A modified side-sensitive synthetic chart to monitor the process mean. *Quality Technology and Quantitative Management*, 15(3), 328-353.

Wisner, P.S. (2009). Statistical process control for quality improvement. *Finance: The Ultimate Resource*, Bloomsbury Press.

Woodall (1986). Weaknesses of the economical design of control charts. *Technometrics*, 28, 408-409.

Wu, Z. & Spedding, T.A. (2000). A synthetic control chart for detecting small shifts in the process mean. *Journal of Quality Technology*, 32(1), 32-38.

Zhang, S. & Wu, Z. (2005). Designs of control charts with supplementary runs rules. *Computers & Industrial Engineering*, 49(1), 76-97.